ELSEVIER

Polymer 41 (2000) 2813–2825

polymer

Microstructural and morphological characteristics of PS–SiO_2 nanocomposites

Ging-Ho Hsiue[a,*], Wen-Jang Kuo[a], Yuan-Pin Huang[b], Ru-Jong Jeng[c]

[a]*Department of Chemical Engineering, National Tsing Hua University, Hsinchu, Taiwan*
[b]*Department of Chemistry, National Chung Hsing University, Taichung, Taiwan*
[c]*Department of Chemical Engineering, National Chung Hsing University, Taichung, Taiwan*

Received 11 January 1999; received in revised form 7 June 1999; accepted 30 June 1999

Abstract

A series of organic–inorganic hybrid materials have been prepared by copolymerizing styrene and alkoxysilane-methacrylate via the sol–gel process. The alkoxysilane-containing copolymer precursors were synthesized by free-radical copolymerization of styrene with an alkoxysilane-containing monomer, methacrylic acid 3-(trimethoxysilyl)propyl ester (MAMSE), at several feeds. The copolymer precursors were then hydrolyzed and condensed to generate PS–SiO_2 hybrid sol–gel materials. The hybrid copolymers possess excellent optical transparency and a nanoscale microphase separation. The copolymer precursors and their hybrid copolymers were characterized by FT-IR spectra, ^{1}H NMR spectra, DSC, and TGA thermograms. Chemical structural effect on the morphology and thermal properties was investigated with SEM, mapping photographs, and high-resolution solid state ^{13}C and ^{29}Si NMR spectra. It was found that compatibility between copolymer and silica mainly comes from incorporating the polymer with silica covalently. Moreover, MAMSE could be hydrolyzed to methacrylic acid and ester-interchanged to silyl methacrylate during heat treatment. This also enhances the compatibility between the copolymer and silica. The thermal properties of the PS–SiO_2 hybrid copolymers are improved as silica content increase. However, the presence of silyl ester groups, which were formed during heat treatment, would reduce the thermal stability of the hybrid copolymers.

Keywords: Nanocomposite; Sol–gel materials; Morphology

1. Introduction

The sol–gel process is of interest in preparing organic–inorganic hybrid materials due to its mild conditions, such as low temperature and pressure [1–5]. The process provides a convenient route to prepare homogeneous hybrid materials, which possess organic and inorganic properties [5,6]. Many researchers [7–12] have demonstrated that monolithic, transparent hybrid materials without macroscopic phase separation can be prepared by properly controlling the condition of hydrolysis and condensation of sol–gel materials such as tetraethoxysilane or tetramethoxysilane (TEOS or TMOS). In these hybrid materials, organic and inorganic constituents can be chemically bonded or just physically mixed.

The specific mechanical and thermal properties of the sol–gel materials are affected by particle sizes and interfacial interaction between the dispersed and the continuous phase [13]. Further, the compatibility of the organic and inorganic hybrid materials are influenced by solvent, coupling agent, aging history, the percent of shrinkage accrued, and the network microstructures [14]. A significant feature to enhance the compatibility in the hybrid materials is the formation of covalent bonding between organic polymers and inorganic components. Not only do the hybrid materials exhibit tunable properties of both organic polymers and inorganic glasses, but also have a blur interface. The structures of the interfacial regions of composites have been studied by Fourier-transform infrared spectroscope (FT-IR) and nuclear magnetic resonance spectroscope (NMR) [15–20]. Moreover, the effects of chemical structure and morphology on the physical characteristics have been investigated by thermal analysis [21–23], mechanical [19,24–26] and viscoelastic [27] properties.

In this study, a series of polystyrene–SiO_2 hybrid copolymers were prepared. Copolymer precursors having trimethoxysilyl-functionality were prepared by free radical copolymerization of styrene with 3-(trimethoxysilyl)propyl mathacrylate (MAMSE). The copolymer precursors were then hydrolyzed and condensed in the presence of an

* Corresponding author. Tel.: +886-35-719-956; fax: +886-35-726-825.

0032-3861/00/$ - see front matter
PII: S0032-3861(99)00478-4

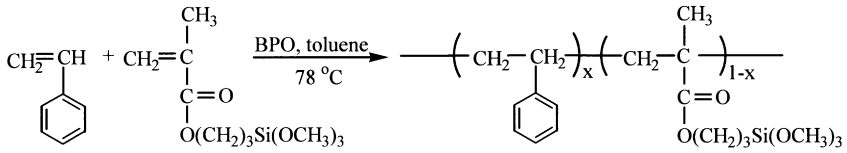

Scheme 1. Synthesis of alkoxysilane-containing polymer precursors.

aqueous HCl catalyst to generate polystyrene–SiO_2 hybrid copolymers. These precursors and hybrid copolymers were characterized with FT-IR, differential scanning calorimeter (DSC), thermogravimetric analysis (TGA), and ^{1}H NMR, spectroscopes. The compatibility of the hybrid copolymers and their relationship between chemical structure and morphology were investigated using scanning electronic microscopy (SEM), mapping, solid state ^{29}Si, and ^{13}C NMR spectroscopes.

2. Experimental

2.1. Materials

Styrene was purchased from Acros Organics Company and purified by treating with 5% aqueous NaOH, drying over anhydrous magnesium sulfate and calcium hydride, followed by distillation under reduced pressure. 3-(Trimethoxysilyl)propyl methacrylate (MAMSE) was purchased from Tokyo Kasei Kogyo Co., Ltd and used as received. Benzoyl peroxide (BPO) was purchased from Lancaster and purified by recrystalization from acetone. Toluene was purchased from Tedia Company Inc. and used as received.

2.2. Synthesis of copolymer precursors

The PS–SiO_2 copolymer precursors were obtained via copolymerization and sol–gel process according to the literature [28,29]. Several precursors were produced via copolymerizations of styrene with 3-(trimethoxysilyl)-propyl methacrylate at various feed compositions. The copolymerization was carried out using BPO as a free radical initiator in a 250-ml three-neck flask at 78°C under nitrogen. The concentration of comonomers was maintained at 2 M in toluene and the reaction time was about 6–24 h depending on the content of 3-(trimethoxysilyl)propyl methacrylate. These copolymer precursors were purified by reprecipitation in hexane. The synthetic route is shown in Scheme 1.

2.3. Preparation of the hybrid sol–gel materials

The PS–SiO_2 hybrid copolymers were prepared via the sol–gel process. The synthetic route is shown in Scheme 2. The PS–SiO_2 copolymer precursors were dissolved in THF solution, and the concentrations were controlled at 20 (W/V)%. A trace of the aqueous solution of hydrochloride was then added. The solution was stirred for 30 min, and then casted onto Teflon®-coated plate. After drying for 2–3 days, transparent films were obtained. Further curing of the glass was performed in an oven at 200°C for 2–4 h. After heat treatment, thermally stable sol–gel films without cracks were obtained.

2.4. Instrumentation and characterization

The chemical structures were identified by FT-IR, solid state ^{29}Si and ^{13}C NMR spectra, which were recorded on a Bio-Rad FT-IR Spectrometer and a Bruker DSX-400WB, respectively. The samples for FT-IR analyses were mixed with KBr powder and pressed into pellets. The thermal properties were characterized by DSC and TGA, which were performed on Seiko DSC 5200 equipped with an Exstar 6000 mode TGA. The DSC and TGA measurements were performed at a heating rate of 10°C/min. The copolymer precursors were measured under nitrogen atmosphere, whereas the hybrid copolymers were measured under air atmosphere. The temperature range for TGA measurements is from 30 to 950°C. The samples for the solid state ^{29}Si NMR and thermal analyses were treated at 200°C for 2–4 h and then ground into fine powder. The morphology of the fractured surfaces of the hybrid materials were observed by SEM and mapping photographs (Hitachi S-2300).

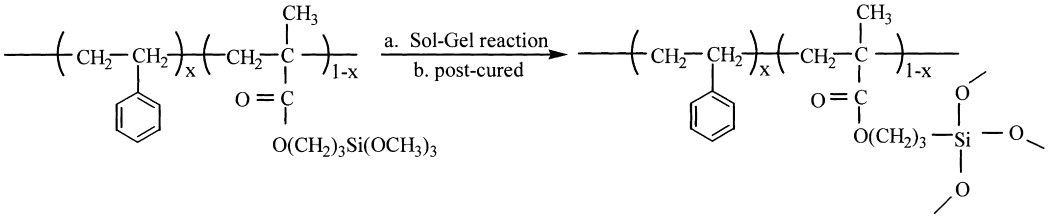

Scheme 2. Preparation of organic–inorganic hybrid film by sol–gel process.

Table 1
Compositions and thermal properties of alkoxysilane-containing polymer precursors

Sample code	The composition of feed (mol.%)		The composition of precursor (mol.%)[a]		T_g (°C)	T_d (°C)[b]
	Styrene	MAMSE	Styrene	MAMSE		
P-S0M10	0	100	0.0	100.0	−26	192
P-S2M8	20	80	26.4	73.6	−10	278
P-S4M6	40	60	44.6	55.4	8	278
P-S6M4	60	40	61.0	39.0	25	322
P-S8M2	80	20	76.2	23.8	48	315

[a] All of compositions of precursors are calculated from the ratios of the ^{1}H NMR-integrated signal of the Si–OCH_3 protons to the aromatic protons.
[b] The thermal degradation temperatures (T_d) are defined as weight loss at 5 wt%, which were performed at heating rate 10°C/min under nitrogen atmosphere.

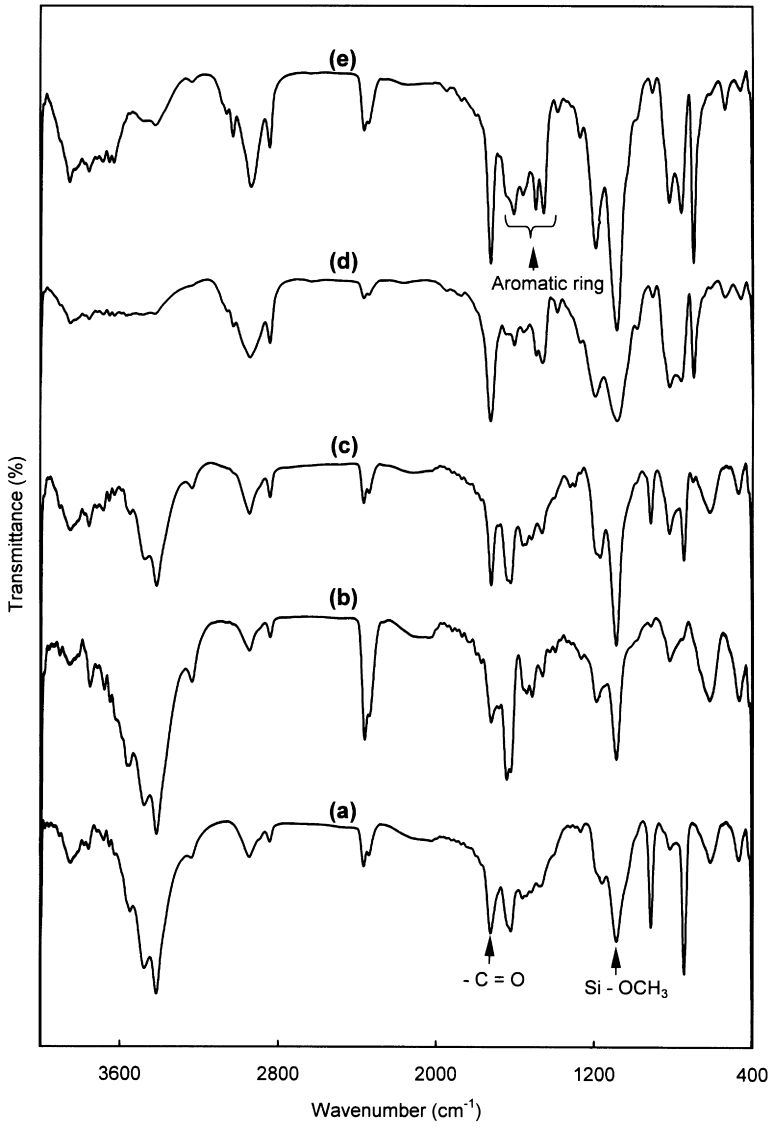

Fig. 1. FT-IR spectra of alkoxysilane-containing copolymer precursors: (a) P-S0M10; (b) P-S2M8; (c) P-S4M6; (d) P-S6M4; and (e) P-S8M2.

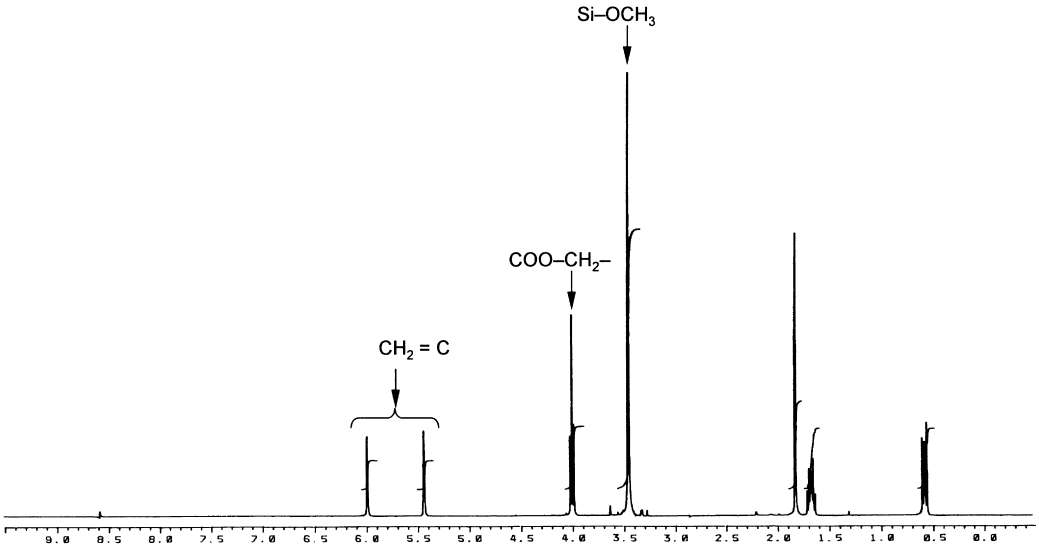

Fig. 2. ^{1}H NMR spectrum of alkoxysilane-containing monomer MAMSE.

3. Result and discussion

3.1. Identification and characterization of copolymer precursors

The PS–SiO_2 copolymer precursors were synthesized via free radical copolymerization of styrene with 3-(trimethoxysilyl)propyl methacrylate according to literature [28,29]. The procedure is schematically described in Scheme 1. The compositions of the copolymer precursors were calculated from ^{1}H NMR spectra and summarized in Table 1. The samples P-S0M10, P-S2M8, P-S4M6, and P-S8M2 represent the copolymer precursors at feed ratios of alkoxysilane-containing monomer MAMSE at 100, 80, 60, 40, and 20 mol.%, respectively.

The structures of the PS–SiO_2 copolymer precursors were

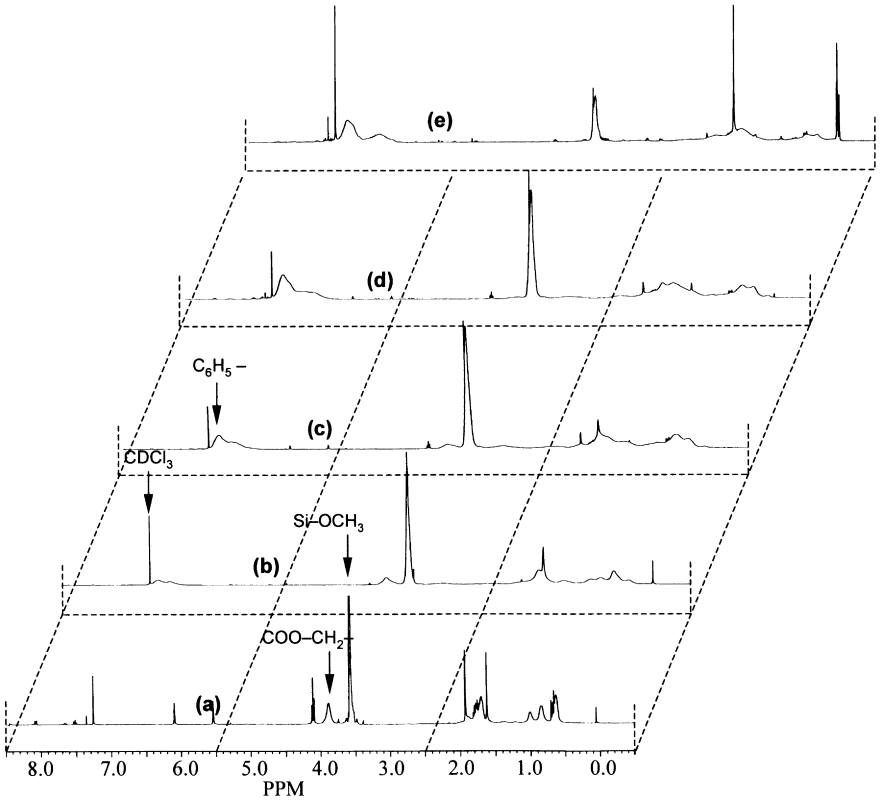

Fig. 3. ^{1}H NMR spectra of alkoxysilane-containing copolymer precursors: (a) P-S0M10; (b) P-S2M8; (c) P-S4M6; (d) P-S6M4; and (e) P-S8M2.

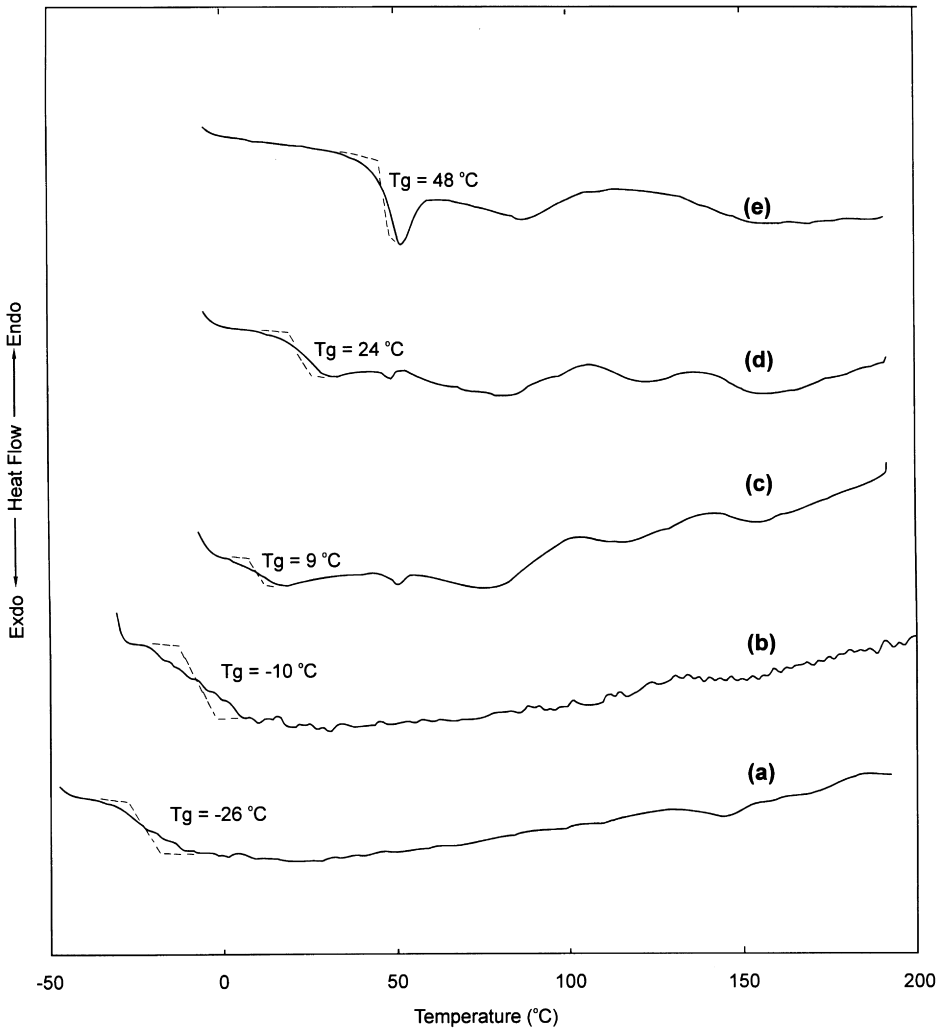

Fig. 4. DSC thermograms of alkoxysilane-containing copolymer precursors with the heating rate 10°C/min under nitrogen atmosphere: (a) P-S0M10; (b) P-S2M8; (c) P-S4M6; (d) P-S6M4; and (e) P-S8M2.

characterized by FT-IR, and ^{1}H NMR spectra. The typical FT-IR spectra for the PS–SiO_2 copolymer precursors are shown in Fig. 1. The characteristic bands of 3-(trimethoxysilyl)propyl methacrylate units appeared at 1736 cm^{-1} for the C=O bond and at 1089 cm^{-1} for the Si–OCH_3 bond [30]. The characteristic bands of the aromatic ring contributing from styrene units are observed at 1604, 1492 and 1450 cm^{-1}. Figs. 2 and 3 show the ^{1}H NMR spectra of the MAMSE and PS–SiO_2 copolymer precursors, respectively. In the ^{1}H NMR spectra (Fig. 2), the chemical shifts appearing between 5.4 and 6.0 ppm can be associated to the vinyl protons in MAMSE. A singlet peak appearing at 3.4 ppm can be assigned to the methyl protons of Si–OCH_3. The triplet peaks appearing at 4.0 ppm correspond to the methylene protons of COO–CH_2–. Fig. 3 shows the ^{1}H NMR spectra of the copolymer precursors. The vinyl protons of the methacrylate peaks appear at 6.0 and 5.4 ppm. Moreover, the chemical shifts of the methylene protons of COO–CH_2– has shifted upfield to 3.5 ppm due to copolymerization. On the contrary, the aromatic protons in the styrene units appear between 7.0 and 7.2 ppm for the copolymer precursors. The copolymer compositions could be estimated from the ratios of the integrated signal of the methyl protons of Si–OCH_3 to the aromatic protons. These results are listed in Table 1.

The thermal properties of the copolymer precursors were characterized by DSC and TGA. Fig. 4 shows the DSC thermogram of the copolymer precursors. The glass transition temperature (T_g) decreased as the MAMSE content increased. This indicates that the pending alkoxysilyl group has a plasticization effect on the copolymer precursors. The TGA thermogram of the copolymer precursors is shown in Fig. 5. The thermal degradation temperature (T_d; 5% weight loss) dramatically increased when styrene was introduced to the MAMSE homopolymer by covalent bonding. The thermal

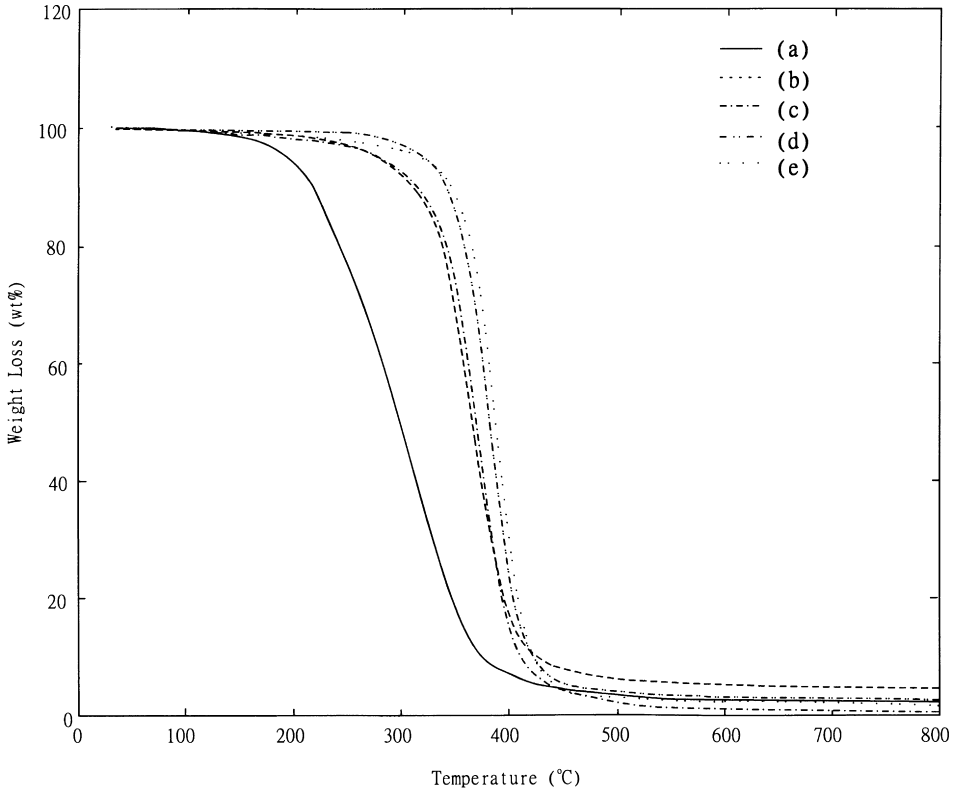

Fig. 5. TGA thermograms of alkoxysilane-containing copolymer precursors with the heating rate 10°C/min under nitrogen atmosphere: (a) P-S0M10; (b) P-S2M8; (c) P-S4M6; (d) P-S6M4; and (e) P-S8M2.

properties of the copolymer precursors are listed in Table 1.

3.2. Identification and characterization of PS–SiO_2 hybrid materials

The PS–SiO_2 hybrid copolymers were prepared via the sol–gel process. To confine the particle size of silica, the PS–SiO_2 copolymer precursors were directly hydrolyzed and condensed in THF solution with a trace of HCl aqueous solution (0.2 M) at room temperature without adding the coupling agent TEOS. The process is shown in Scheme 2. The thermal stability for the hybrid copolymers were enhanced by further thermal treatment at 200°C for 2–4 h after gelling and drying at room temperature. All of the hybrid copolymers exhibited excellent optical transparency.

Fig. 6 shows the FT-IR spectra of the PS–SiO_2 hybrid copolymers after heat treatment. The characteristic absorption bands of Si–OCH_3 at 1088 cm^{-1} in the copolymer precursors became vague, whereas the characteristic absorption bands of Si–O–Si bond around 1000–1200 cm^{-1} emerged and their intensities increased with increasing MAMSE content. This implies that a more complete sol–gel reaction occurred during heat treatment.

After heat treatment, the thermal stability increased significantly. The T_gs of the PS–SiO_2 hybrid copolymers increased with increasing MAMSE content (Fig. 7). This result is different from that of the copolymer precursors. This is due to the fact that the plasticizing trimethoxysilyl groups have transformed to silica network during the sol–gel process. The TGA thermogram for all hybrid copolymers is shown in Fig. 8. The silica contents in the hybrid copolymers were determined from the residual weight at 950°C in the TGA thermograms under air atmosphere and listed in Table 2. The samples H-S0M10, H-S2M8, H-S4M6, and H-S8M2 represent the copolymers resulted from thermal treatment of the precursors P-S0M10, P-S2M8, P-S4M6, and P-S8M2, respectively. The thermal degradation behaviors of the hybrid copolymers were divided into two stages. The primary degradation stage could be caused by the cleavage of copolymer chains, and the secondary degradation stage could be brought about by further oxidization of silicate. The T_ds of the hybrid copolymers are also listed in Table 2. The T_d of the hybrid homopolymer H-S0M10 increased when the homopolymer precursor P-S0M10 was hydrolyzed and condensed. On the contrary, T_d of the hybrid copolymer increased as compared to the homopolymer, when low content of styrene was covalently incorporated. However, as the styrene content increased, T_ds decreased. This phenomenon is probably due to variation in morphology or chemical structures of the hybrid copolymers.

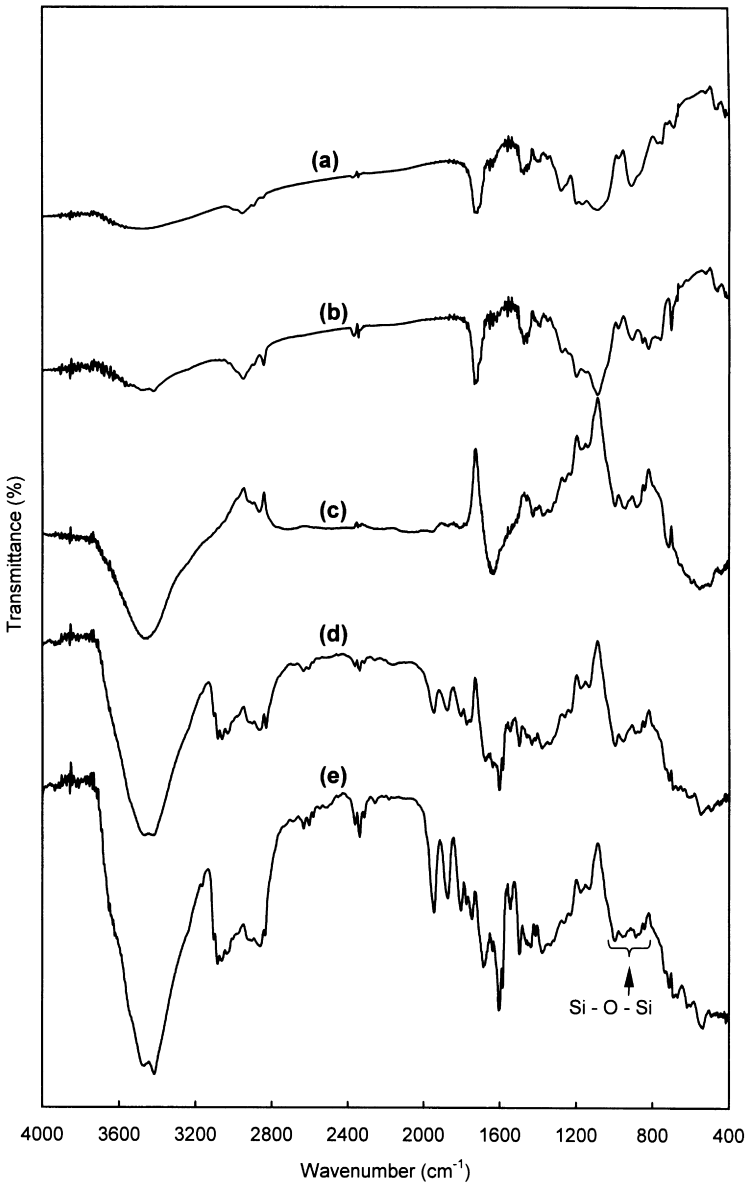

Fig. 6. FT-IR spectrum of silica-containing hybrid copolymers: (a) H-S0M10; (b) H-S2M8; (c) H-S4M6; (d) H-S6M4; and (e) H-S8M2.

3.3. Morphology study

The compatibility between the organic copolymer and silica has a great effect on the thermal, mechanical and optical properties. To investigate the distribution of silica and microphase separation in the hybrid matrix, the morphology of the fractured surfaces was observed by SEM (Fig. 9) and a mapping technique (Fig. 10). A planar fractured surface was observed in low magnification (3K×). Fig. 9 shows a higher magnification SEM micrograph (25K×). In this photograph, brittle hybrid structures were observed. Moreover, microphase separations were also observed on the fractured surfaces of these hybrid matrixes. According to the micrographs, the particle sizes are in the nanoscale. In mapping photographs (Fig. 10), the silica particles are uniformly dispersed in the copolymer matrix. These results show that silica networks are restrained under molecular level in the PS–SiO_2 hybrid copolymers.

3.4. Relationship between morphological characteristics and microstructure

To investigate the effect of chemical structure of the PS–SiO_2 hybrid copolymers on morphology and thermal properties, solid state ^{29}Si and ^{13}C NMR techniques were applied. Fig. 11 shows the solid state ^{29}Si NMR spectra of the hybrid copolymers. In the spectra, the chemical shift of

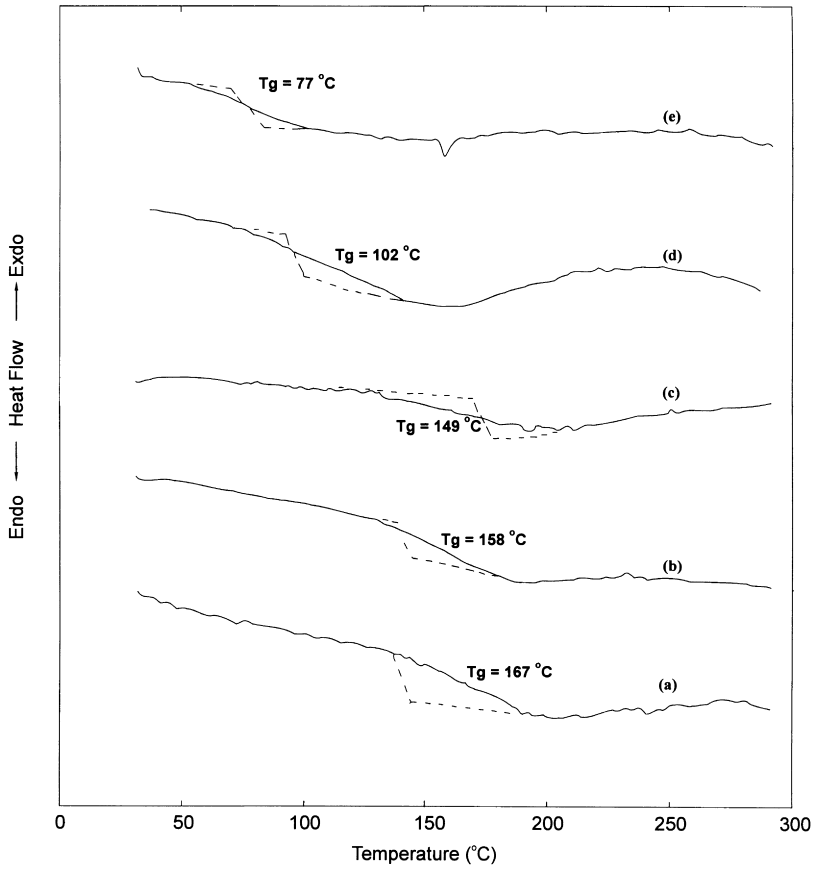

Fig. 7. DSC thermogram of silica-containing hybrid copolymers with the heating rate 10°C/min under nitrogen atmosphere: (a) H-S0M10; (b) H-S2M8; (c) H-S4M6; (d) H-S6M4; and (e) H-S8M2.

unsubstituted, mono-, di-, and tri-substituted siloxanes appear at −42, −50, −60, and −67 ppm, respectively [20]. For the hybrid copolymers with high MAMSE content, the mono- and di-substituted silicates are dominant. Moreover, the unsubstituted silicate in the hybrid copolymer increases with decreasing MAMSE content. This is due to the fact that the polymer covalently incorporated with silica confines aggregation and condensation of silanol. Therefore, mono- and di-substituted silicates dominate the chemical structure, whereas tri-substituted silicate appears vaguely at solid ^{29}Si NMR spectra. Moreover, hydrolysis process is restricted due to the large amount of hydrophobic copolymer chain, when the MAMSE content is low. This leads alkoxysilane to the formation of un-, mono- and di-substituted silica in the hybrid copolymers.

To investigate the microstructure of the hybrid silica, solid state ^{13}C NMR was applied. Fig. 12 shows the ^{13}C NMR spectrum of the monomer MAMSE. In the spectrum, the chemical shift for the trimethoxysilyl group appears at 50 ppm, whereas the carboxylate group has a chemical shift at 167 ppm. Fig. 13 shows the solid state ^{13}C NMR spectra of the PS–SiO_2 hybrid copolymers. For the hybrid copolymers, the chemical shift of the trimethoxysilyl group appears at 45 ppm. This implies that the trimethoxysilyl group does not hydrolyze and condense completely. The chemical shift for the carboxylate group has shifted downfield to 180 ppm due to the formation of the hybrid homopolymer (H-S0M10), whereas other chemical shifts of carboxylate group appear at 198 and 217 ppm for those hybrid copolymers, and their intensities are increased with decreasing MAMSE content. This implies that the carboxylate group transforms to methacrylic acid ($\delta = 217$ ppm) and ester-interchanges ($\delta = 198$ ppm) with silanol to silyl methacrylate at lower MAMSE content. This indicates that silane might not be easily hydrolyzed with inorganic acid at low MAMSE content. Consequently, the trimethoxysilyl groups are still present in the hybrid copolymers after curing. Moreover, the steric hindrance effect of the organic copolymer, and the chemical bonding effect restrict the aggregation and condensation of silanol. Instead of the sol–gel process, hydrolysis of methacrylate and ester interchange processes occur at high temperature heat treatment. A similar phenomenon was also observed in acid-catalyzed hydrolysis and condensation reactions [31]. Moreover, the thermal stabilities of the hybrid copolymers are influenced by ester-interchanging methacrylate with silanol. For the copolymer precursors, thermal degradation is mainly caused

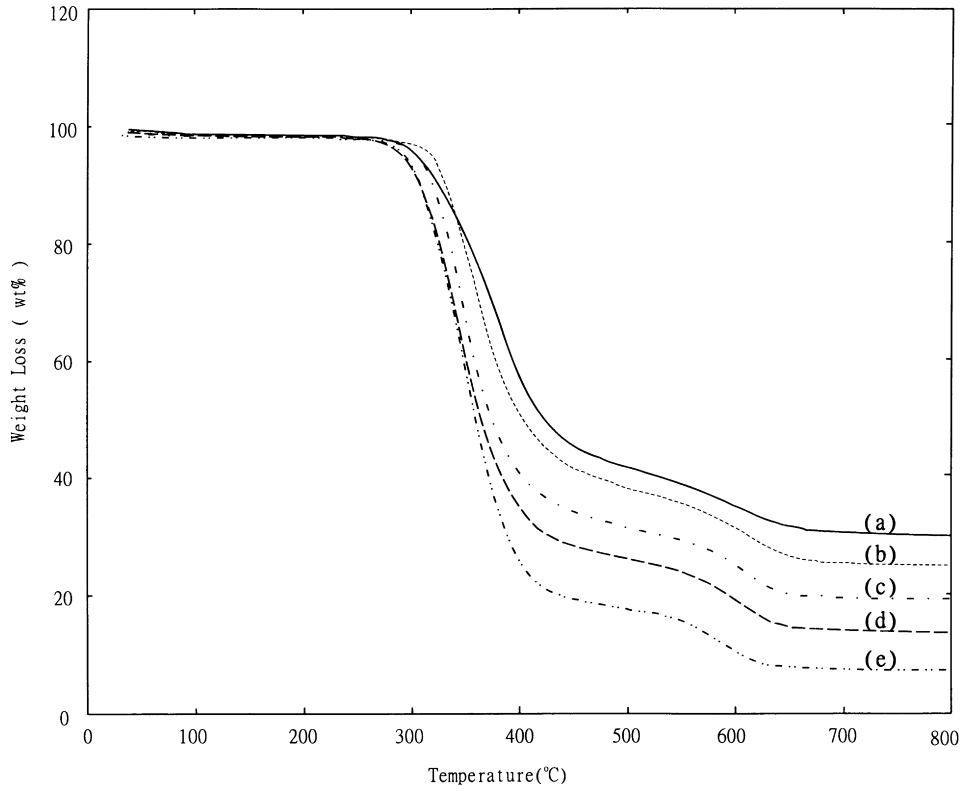

Fig. 8. TGA thermograms of silica-containing hybrid copolymers with the heating rate 10°C/min under air atmosphere: (a) H-S0M10; (b) H-S2M8; (c) H-S4M6; (d) H-S6M4; and (e) H-S8M2.

by the cleavage of methacrylate. Thermal stability was enhanced by introducing styrene to polymers and increased with decreasing MAMSE content. For hybrid copolymers, thermal stability was enhanced by the formation of silica. However, unstable silyl esters are generated during heat treatment, and the content of silyl esters is increased with decreasing MAMSE content. So thermal degradation temperature of the hybrid copolymers is decreased as decreasing MAMSE content.

Based on the above, the compatibility of the PS–SiO_2 hybrid copolymers can be enhanced via incorporating polymer matrix with inorganic silica covalently. The chemical bonding not only restricts the migration of inorganic silicates but also hinders the aggregation of silanol. Moreover, for the PS–SiO_2 hybrid copolymers with low MAMSE content, better compatibility between organic polymer matrix and inorganic silica was brought about via polar interaction between methacrylic acid and silicate, chemical bonding between copolymer backbone and grafted silicate, and ester interchange between mathacrylate and silicate. The thermal stabilities of the hybrid copolymers can be enhanced via the formation and uniformly dispersion of silica. When the MAMSE content is high, the silanol is mainly transformed to the Si–O–Si structure. Therefore, the thermal stability of the copolymer precursors can be further improved. However, the silanol is mainly

Table 2
Thermal properties and residual SiO_2 content of silica-containing hybrid polymers

Sample code	The composition of feed (mol.%)		T_g (°C)	T_d (°C)[a]	Residual SiO_2 contents (wt%)[b]
	Styrene	MAMSE			
H-S0M10	0	100	167	306	29.6
H-S2M8	20	80	158	320	25.4
H-S4M6	40	60	149	306	20.0
H-S6M4	60	40	102	301	15.0
H-S8M2	80	20	77	295	8.7

[a] The thermal degradation temperatures (T_d) are defined as weight loss of TGA thermogram at 5 wt%.
[b] Residual SiO_2 contents are obtained from TGA thermograms, which were performed at heating rate 10°C/min under air atmosphere.

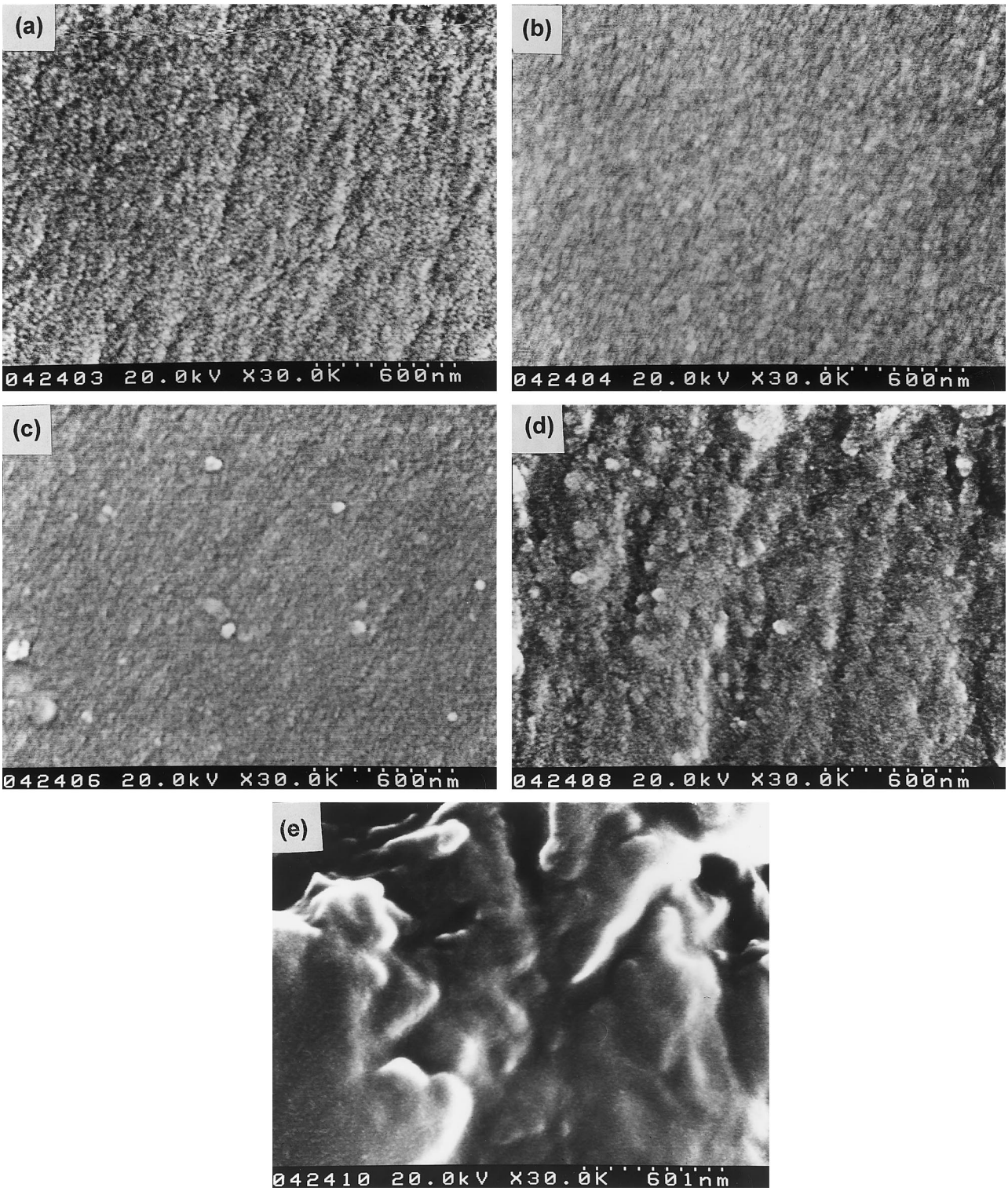

Fig. 9. SEM photographs of silica-containing hybrid copolymers: (a) H-S0M10; (b) H-S2M8; (c) H-S4M6; (d) H-S6M4; and (e) H-S8M2.

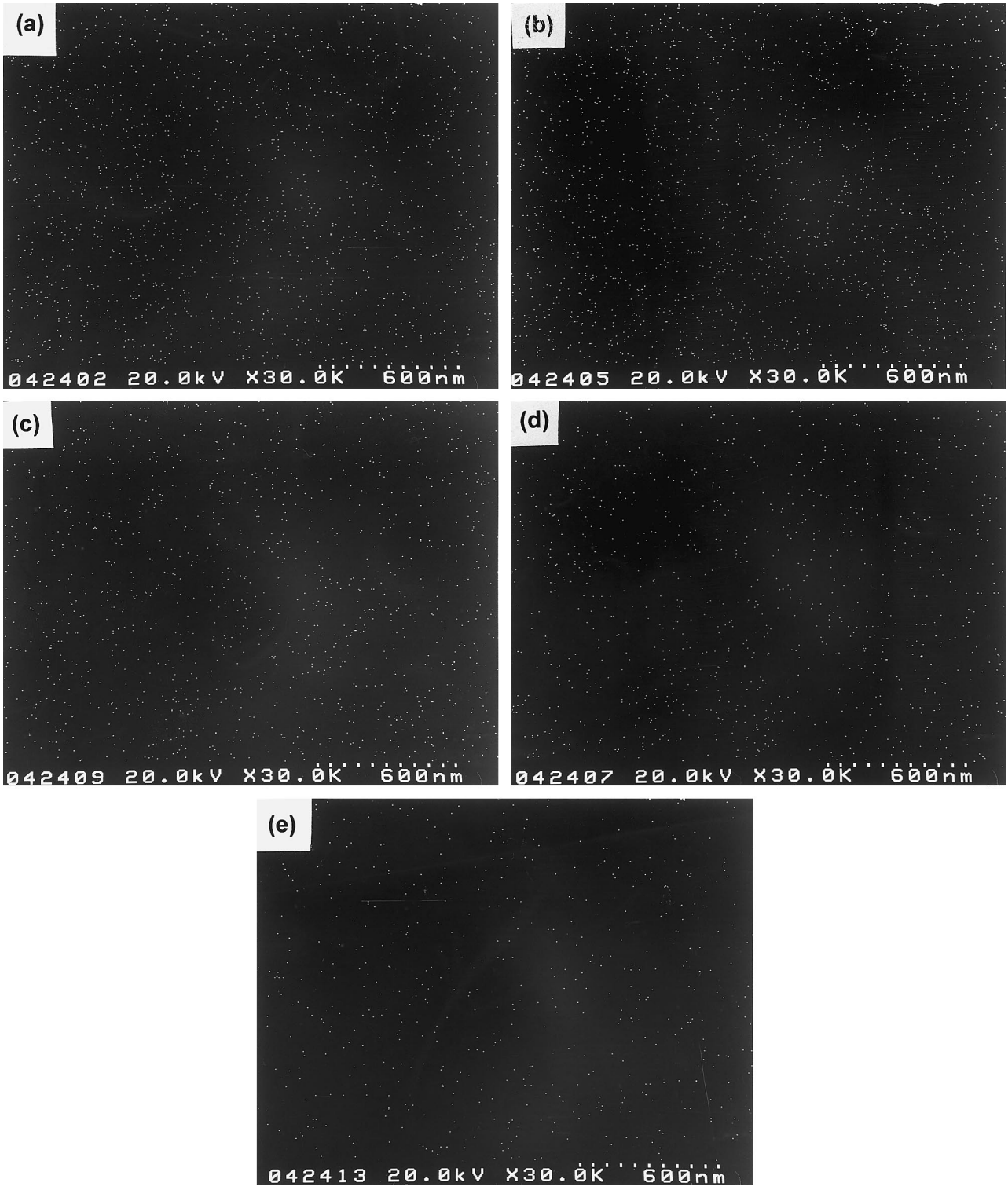

Fig. 10. Mapping photograph of silica-containing hybrid copolymers: (a) H-S0M10; (b) H-S2M8; (c) H-S4M6; (d) H-S6M4; and (e) H-S8M2.

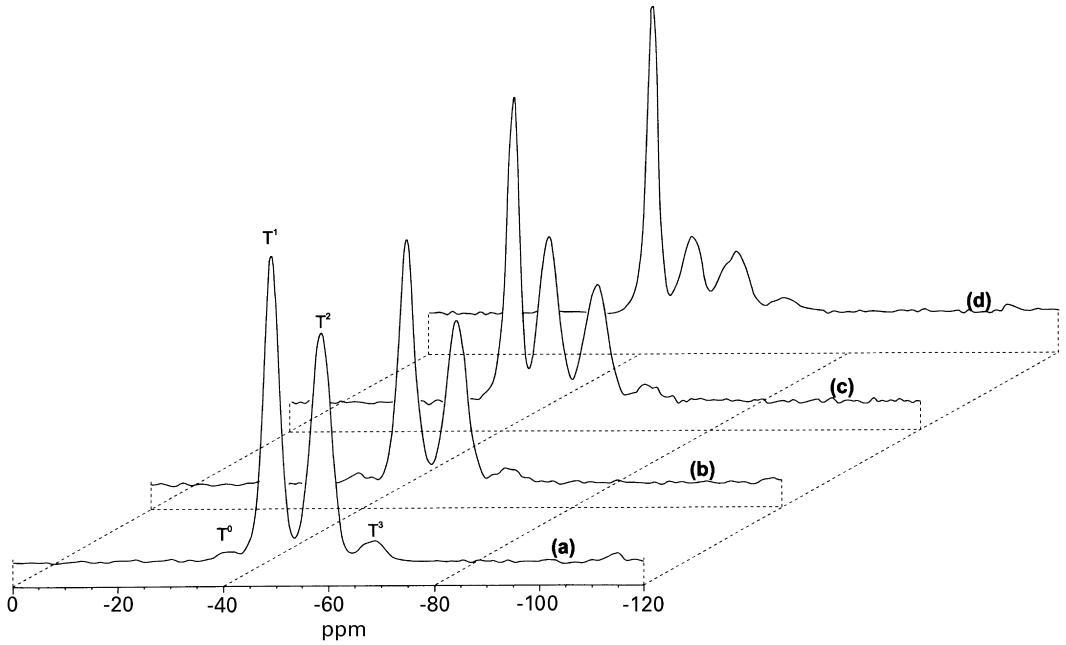

Fig. 11. Solid state ^{29}Si NMR spectra of silica-containing hybrid copolymers: (a) H-S0M10; (b) H-S2M8; (c) H-S4M6; and (d) H-S8M2.

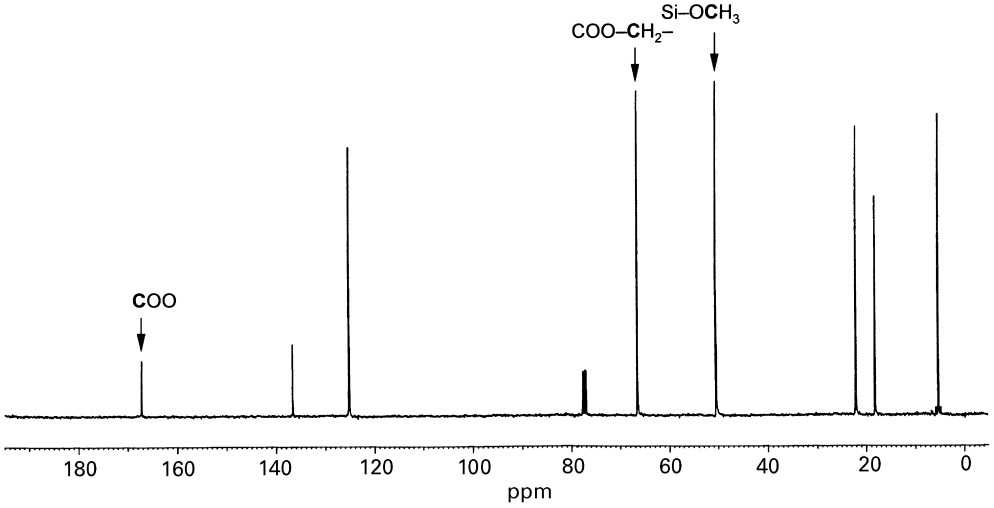

Fig. 12. ^{13}C NMR spectrum of alkoxysilane-containing monomer MAMSE.

transformed to the COO–Si structure due to ester interchange when MAMSE content is low. Therefore, the thermal stability of the copolymer precursor (low MAMSE content) is more stable than the heat-treated hybrid copolymers.

4. Conclusion

In this article, a series of alkoxysilane-containing prepolymers were prepared by a copolymerizing alkoxysilane-containing monomer and styrene. After curing, the hybrid copolymers possessed excellent miscibility. The silica particles were uniformly dispersed in the copolymer matrix, and their sizes were in the nanoscale. Miscibility between the silica and the copolymer was enhanced by covalent bonding between the organic and inorganic components, steric hindrance of the copolymer backbone as well as hydrolysis and ester-interchange of methacrylate. The thermal stability of the hybrid copolymers was also increased with increasing silica content. However, the thermally unstable silyl ester groups reduced the stability

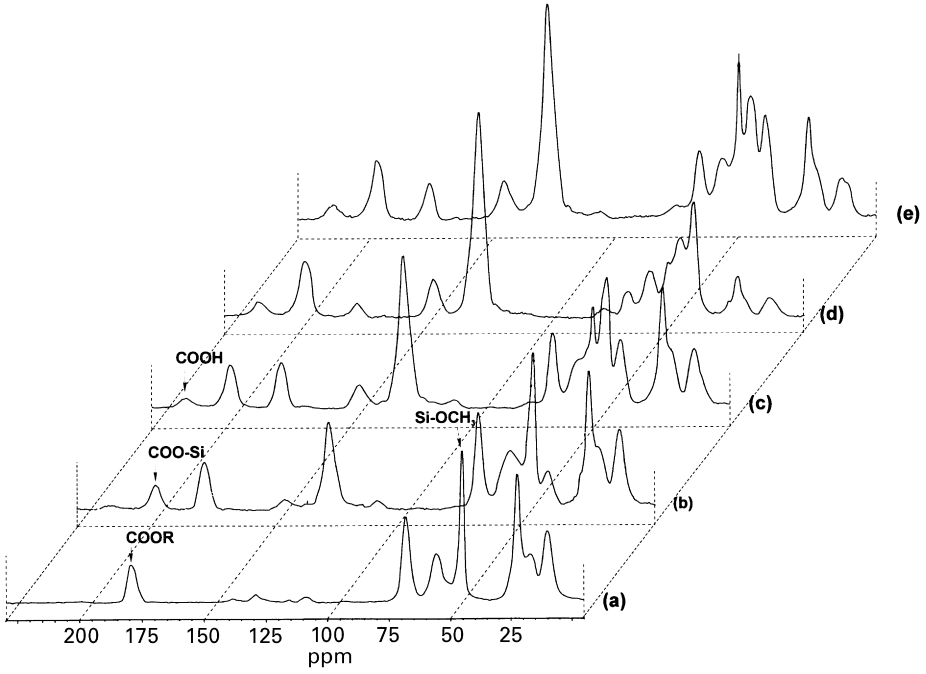

Fig. 13. Solid state ^{13}C NMR spectra of PS–SiO_2 hybrid copolymers: (a) H-S0M10; (b) H-S2M8; (c) H-S4M6; (d) H-S6M4; and (e) H-S8M2.

of the hybrid copolymer when MAMSE content was low.

Acknowledgements

The authors thank the National Science Council of Republic of China for financial support of this work (Grant NSC 87-2216-E007-032).

References

[1] Dislich H. Angew Chem Int Ed Engl 1971;10:363.
[2] Mackenzie JD. J Non-Cryst Solids 1982;48:1.
[3] Hench LL, West JK. Chem Rev 1990;90:33.
[4] Brinker CJ, Scherer GW. J Non-Cryst Solids 1985;70:301.
[5] Mark JE, Lee CY, Biancone PA. Hybrid organic–inorganic composites, ACS Symposium series 585. Washington, DC: American Chemical Society, 1995.
[6] Novak BM. Adv Mater 1993;5:422.
[7] Kawaguchi T, Hishikura H, Iura J, Kokuba Y. J Non-Cryst Solids 1984;63:61.
[8] Wei Y, Yang D, Jang L, Hutchins MK. J Mater Res 1993;8:1143.
[9] Wojcik AB, Klein LC. J Sol–Gel Sci Technol 1995;5:77.
[10] Sharp KG, Michalczyk MJ. J Sol–Gel Sci Technol 1997;8:541.
[11] Coltrain BK, Landry CJT, O'Reilly JM. Chem Mater 1993;5:1445.
[12] McCarthy DW, Mark JE, Schaefer DW. J Polym Sci Part B: Polym Phys 1998;36:1167.
[13] Landry CT, Coltrain BK, Brady BK. Polymer 1993;33:1486.
[14] McCarthy DW, Mark JE, Schaeffer DW. J Polym Sci Part B: Polym Phys 1998;36:1167.
[15] Harris RK, Robins ML. Polymer 1978;19:1123.
[16] Poxuviel JC, Boilot JP, Beloeil JC, Lallemand JY. J Non-Cryst Solids 1987;89:345.
[17] Witte BMD, Commers D, Uytterhoeven JB. J Non-Cryst Solids 1996;202:35.
[18] Prabakar S, Assink RA, Raman NK, Myer SA, Brinker CJ. J Non-Cryst Solids 1996;202:53.
[19] Yang JJ, El-Nahhal IM, Chuang IS, Maciel GE. J Non-Cryst Solids 1997;212:281.
[20] Joseph R, Zhang S, Ford W. Macromolecules 1996;29:1305.
[21] Stefanithis D, Mauritz KA. Macromolecules 1990;23:2397.
[22] Wei Y, Yang D, Bakthavatchalam R. Mater Lett 1992;13:261.
[23] Chen W, Fang H, He D, Ye C. J Appl Polym Sci 1996;67:139.
[24] Becker C, Krug H, Schmidt H. J Sol–Gel Sci Technol 1997;8:625.
[25] Ahmad Z, Sarwar MI, Mark JE. J Appl Polym Sci 1997;63:1352.
[26] Huang ZH, Dong JH, Qiu KY, Wei Y. J Appl Polym Sci 1997;66:853.
[27] Nicolai T, Randrianantopandro H, Prochazka F, Durand D. Macromolecules 1997;30:5897.
[28] Rao VL, Babu GN. Eur Polym J 1989;25:605.
[29] Wei Y, Yang D, Tang L, Hutchins M-GK. J Mater Res 1993;8:1143.
[30] Daimay LV, Norman BC, William GF, Jeanette GG. The handbook of infrared and Raman characteristic frequencies of organic molecules, Boston: Academic, 1995.
[31] Sharp KG. J Sol–Gel Sci Technol 1994;2:35.